Stuart J. Williams

Department of Mechanical Engineering, University of Louisville, Louisville, KY, USA

Received July 15, 2012
Revised January 21, 2013
Accepted February 6, 2013

Research Article

Enhanced electrothermal pumping with thin film resistive heaters

This work demonstrates the use of thin film heaters to enhance electrothermal pumping in microfluidic systems. Thin film heating electrothermal pumping is more efficient than Joule heating alone. Numerical simulations of an asymmetric electrode array are performed to demonstrate the advantages of incorporating thin film heaters. This specific simulation shows that thin film heater electrothermal pumping provides approximately two and one-half times more volumetric flow than Joule heating alone for the same input power to both systems. In addition, external heating allows for electrothermal pumping to be applicable to low conductivity media.

Keywords:
Electro-osmosis / Electrothermal / Joule heating / Microfluidics / Pumping
DOI 10.1002/elps.201200377

1 Introduction

The advantages of lab-on-a-chip technologies are numerous, including the significant reduction of sample size and reagent size, very short reaction and analysis time, high throughput, and portability. Electrokinetic methods offer the advantages of no moving parts, straightforward fabrication, ease of microsystem integration, and resistance to particulate contamination. However, the application of high voltages can produce adverse effects like bubble generation and pH gradients. The incorporation of microelectrode features, though, can produce high electric fields at lower voltages, which can be controlled with commercially available bench-top AC signal generators. The two most extensively investigated AC electrokinetic fluid pumping mechanisms are electrothermal pumping and AC electro-osmosis (ACEO). In electrothermal fluid pumping, the applied electric field acts upon dielectric gradients produced from nonuniform heating of the liquid (arising from Joule heating of the liquid itself and/or heating from external elements) leading to bulk fluid motion [1–4]. In ACEO, the electric field induces mobile charges at the interface between the fluid and electrode, and the tangential component of the applied field acts upon these charges resulting in a fluid slip condition on the electrode surface [5–8]. However, electro-osmotic pumping (DC) and ACEO are not as effective as electrothermal pumping for microsystems at high fluid conductivities [9–13], especially for biologically relevant media whose conductivity is on the order of 1 S/m [14]. Therefore, electrothermal hydrodynamics are important for the development of biological microsystems.

There are several disadvantages in current electrothermal pumping designs where a single set of electrodes are used to simultaneously apply the electric field and generate Joule heating. First, it is impossible to alter the electric field independently from Joule heating, and vice versa. Second, for low conductivity media higher voltages are required to generate sufficient Joule heating for electrothermal motion. Joule heating scales with conductivity and the square of the applied field (σE^2) [13]. For example, the amount of heat generated when an electric field is applied to 1.0 S/m media is 100 times greater than when the same field is applied to 0.01 S/m media.

The incorporation of external heating components would enable independent control of heating separate from the electric field. Illumination is one potential source of external heating for electrothermal flow. Fluid can absorb the illumination directly or indirectly through light absorption of the electrode or substrate [1]. Electrothermal fluid motion using highly focused laser beams as the external heating source has been demonstrated [15–17]. Optically based external heating, though dynamic, is not easily portable and it does not have high heating efficiencies.

This work communicates the concept of using thin film resistive heaters as an external heating source for electrothermal pumping. Numerical simulations are used to convey the advantages of this type of system over existing electrothermal pumping methodologies. Thin film heaters have nearly 100% thermal efficiencies (electrical energy conversion to heat energy), which is greater than optically induced heating. Thin film heater fabrication is a well-established technique that can be integrated with microsystems. Such heaters have been used in lab-on-a-chip devices for thermopneumatic pumps

Correspondence: Dr. Stuart J. Williams, Department of Mechanical Engineering, University of Louisville, 200 Sackett Hall, Louisville, KY 40292, USA
E-mail: stuart.williams@louisville.edu
Fax: +1-502-852-6053

Abbreviation: ACEO, AC electro-osmosis

Colour Online: See the article online to view Figs. 1 and 2 in colour.

[18], DNA amplification [19], and chemical sensor research [20]. For most applications uniform heating is desired. For this work, though, nonuniform heating is needed to drive electrothermal pumping.

This manuscript compliments earlier experimental work using independently controlled thin film heaters to create electrothermal fluid circulation in a uniform electric field [21]. However, no bulk fluid pumping was demonstrated, nor expected, in the previous work. Numerical simulations herein demonstrate the benefits of thin film designs and provide the methodology for the design and analysis of such microfluidic systems.

2 Materials and methods

2.1 Theory

Electrothermal flows are generated from the interaction of the electric field with nonuniform permittivity and conductivity induced by temperature gradients. The governing equations for this system begins with Gauss's law and the charge conservation equation:

$$\rho_q = \nabla \cdot (\varepsilon \boldsymbol{E}) \tag{1}$$

$$\partial\rho_q/\partial t + \nabla \cdot \left(\sigma \boldsymbol{E} + \rho_q \boldsymbol{u}\right) = 0 \tag{2}$$

$$\nabla \times \boldsymbol{E} = 0 \tag{3}$$

where ρ_q is the charge density, ε is the permittivity of the fluid, $\boldsymbol{E}$ is the electric field, σ is the conductivity of the medium, and $\boldsymbol{u}$ is the fluid velocity. The convection current term in Eq. (2), $\rho_q \boldsymbol{u}$, can be ignored since the electrical Reynolds number (Re_{el}) for a characteristic velocity, u_o, and a characteristic length, L, is $Re_{el} = (u_o \varepsilon)/(\sigma L) << 1$.

The electrical force density ($\boldsymbol{f}_e$) acting on an incompressible fluid media is given by [22]:

$$\boldsymbol{f}_e = \rho_q \boldsymbol{E} - \frac{1}{2} |\boldsymbol{E}|^2 \nabla\varepsilon \tag{4}$$

The first and second terms on the right hand side of the equation are Coulomb and dielectric forces, respectively.

The fluid velocity is governed by the Navier-Stokes equation for low Reynolds number flows. For steady state, this equation simplifies to:

$$0 = -\nabla p + \mu\nabla^2 \boldsymbol{u} + \boldsymbol{F} \tag{5}$$

and is used in conjunction with mass conservation for an incompressible fluid:

$$\nabla \cdot \boldsymbol{u} = 0, \tag{6}$$

where p is the pressure, μ is the viscosity of the fluid, and $\boldsymbol{F}$ is the sum of the electrothermal force and the buoyancy force. The buoyancy force is given as $\boldsymbol{F}_b = \Delta\rho_m \boldsymbol{g}$, where ρ_m is the fluid density (998 kg/m^3), and $\boldsymbol{g}$ is gravity (9.81 m/s^2). The change in fluid density is $\Delta\rho_m = \rho_m(T_o)(T - T_o)\beta$ where T is temperature, T_o is the reference temperature, and β is the coefficient of thermal expansion (10^{-3} °C^{-1}). Reynolds numbers for such systems are typically low with $Re = \rho_m u_o L/\eta << 1$.

The temperature field is determined by the Joule heating equation:

$$\rho_m c_p \left(\partial T/dt + (\boldsymbol{u} \cdot \nabla)\, T\right) = \nabla \cdot (k\nabla T) + \sigma |\boldsymbol{E}|^2 \tag{7}$$

where k is the fluid heat conductivity, c_p is the fluid heat capacitance, and $\sigma|E|^2$ is the Joule heating term. For high AC frequencies this equation can be simplified to steady state [7]. Thermal convection can be neglected for small thermal Peclet number, $Pe_T = \rho_m c_p u_o L/k << 1$. Assuming constant medium thermal conductivity, Eq. (7) simplifies in terms of time-averaged Joule heating:

$$0 = k\nabla^2 T + \frac{1}{2}\sigma |\boldsymbol{E}|^2 \tag{8}$$

From this point, there are two methodologies of conducting numerical simulations for electrothermal flows. The first method [1, 2, 7, 13] assumed small temperature gradient approximations and scaling law simplifications. The resulting system of equations was solved sequentially as the electrical equation was not coupled with the thermal equation. In this approximation method, the changes in fluid properties were assumed to be small. Using this method, a direct relationship between the fluid velocity and voltage could be determined. For Joule heating systems the electrothermal fluid velocity scales as σE^4 [13]; however, for external sources of heat fluid velocity scales as σE^2.

Recent work by Loire et al. [4, 23], demonstrated that for high temperatures, electrothermal coupling cannot be neglected. Thermoelectric coupling alters the electric field, especially at high temperatures. In addition, their numerical model incorporated temperature dependent parameters (fluid density, viscosity, permittivity, and conductivity). Strong thermoelectric coupling and the temperature dependent variables demonstrated electrothermal fluid velocity scaling of σE^κ with $\kappa > 4$ for high voltages and high fluid conductivities. They concluded that their model should be used for a general temperature increase above 5°C. Therefore, their method was chosen for numerical simulations herein.

The coupled electric and thermal equations from Loire, et al. [4] were derived from the previous electrical Eqs. (1–3), resulting in:

$$\nabla^2 V = \gamma \cdot \nabla V \tag{9}$$

$$\boldsymbol{E} = -\nabla V \tag{10}$$

where $\gamma = -c_\sigma \nabla T$ for $\omega\tau << 1$ and $\gamma = -c_\varepsilon \nabla T$ for $\omega\tau >> 1$. The applied AC frequency is given as $\omega = 2\pi f$. The charge relaxation time of the fluid is $\tau = \varepsilon/\sigma$. Constants c_ε and c_σ are linear approximations of the temperature dependence of

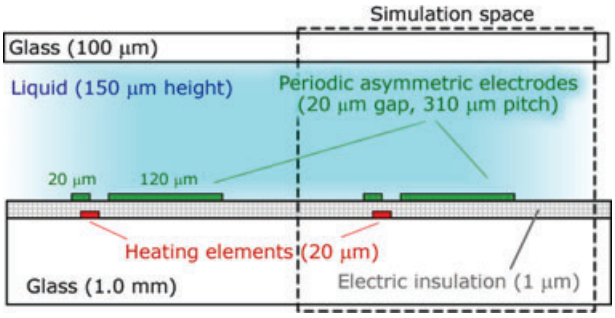

Figure 1. The geometry of the periodic asymmetric electrothermal pump and location of the thin film heater. This figure is not drawn to scale.

the electrical permittivity and conductivity, respectively, with $c_\varepsilon = \frac{1}{\varepsilon}\frac{\partial \varepsilon}{\partial T} \approx -0.004^\circ\mathrm{C}^{-1}$ and $c_\sigma = \frac{1}{\sigma}\frac{\partial \sigma}{\partial T} \approx 0.02^\circ\mathrm{C}^{-1}$.

These equations are used in conjunction with Eqs. (5) and (6) where the fluid body force is $\boldsymbol{F} = \boldsymbol{f}_e + \boldsymbol{F}_b$. The time averaged electrothermal fluid body force is given by [4]:

$$\boldsymbol{f}_e = \frac{1}{2}\varepsilon\left[(c_\varepsilon - c_\sigma)\frac{(\nabla T \cdot E)}{1+(\omega\tau)^2}\boldsymbol{E} - \frac{1}{2}c_\varepsilon \nabla T\,|\boldsymbol{E}|^2\right] \quad (11)$$

For high frequencies ($\omega\tau >> 1$) the Coulomb term becomes negligible in comparison to the dielectric term. For low frequencies ($\omega\tau << 1$) the Coulomb term simplifies as the denominator approaches a value of one.

It is assumed that there is no time phase shift, or a time phase shift of $\pi/2$, and therefore the imaginary part of the electric field is zero. Traveling wave electrothermal pumping has been demonstrated with a series of out-of-phase electrodes [3, 24, 25], but will not be addressed here.

Fluid viscosity, permittivity, and conductivity are temperature dependent. Using their linear approximation, permittivity is $\varepsilon(T) = \varepsilon(T_o)(1 + c_\varepsilon(T - T_o))$ and conductivity is $\sigma(T) = \sigma(T_o)(1 + c_\sigma(T - T_o))$. Viscosity is highly temperature dependent and its value (at a pressure of 1 atm) is approximated with [26]:

$$\ln\left(\mu/\mu_o\right) = -1.704 - 5.306\left(273/T\right) + 7.003\left(273/T\right)^2 \quad (12)$$

where T is in degrees Kelvin and $\mu_o = 0.001788$ kg/(m s). The thermal conductivity of the liquid is assumed constant as its value varies approximately 0.2% per °C.

2.2 Numerical simulation

To illustrate the advantages of thin film-based electrothermal pumping, a comparative numerical analysis is conducted herein. A planar, periodic, interdigitated, asymmetric electrode layout is a traditional electrothermal pump design [24, 27]. The chosen electrode geometry for this study (Fig. 1) was borrowed from recent work by Zhang, et al. [24]. A narrow electrode (20 μm) is separated from a wide electrode (120 μm) with a 20-μm gap. A 150-μm gap separates subsequent electrode pairs. The electrodes are 100 nm thick

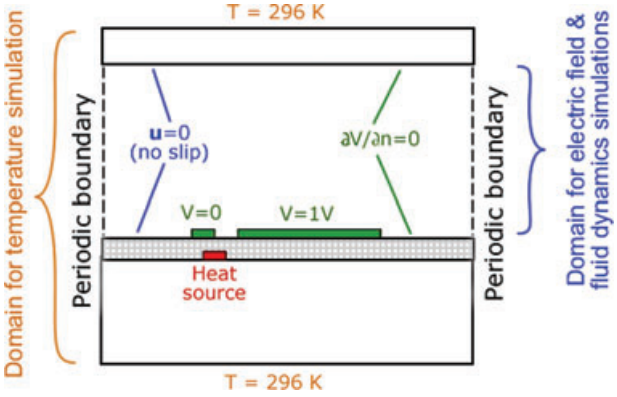

Figure 2. The numerical simulation space and assigned boundary conditions for the electrical, temperature, and fluid velocity models. This figure is not drawn to scale.

on a 1.0 mm glass ($k_g = 1.0$ W/K m) substrate. Water ($k = 0.6$ W/K m) fills a microfluidic channel that is 150 μm in height and is capped with a glass coverslip (100 μm thick). The fluid electrical permittivity is $\varepsilon_r = 80$, where $\varepsilon = \varepsilon_r\varepsilon_o$ (ε_o is permittivity of free space).

The thin film heater electrothermal pump design is shown in Fig. 1. The heater (20 μm wide) is centered at the inside edge of the 20 μm electrode. The heater is embedded in the glass substrate, separated from the above pumping electrodes with a 1.0-μm-thick electric insulation (whose properties are modeled as glass).

The periodic 2D numerical simulation was conducted using COMSOL Multiphysics that incorporated the electrical, thermal, and fluid models. First, the coupled electrical and thermal solutions were determined. Their solutions were used to solve for the resultant fluid velocity. The boundary conditions for the simulation space are shown in Fig. 2. The vertical boundaries are periodic for all three models. The electrical and fluid dynamics simulation space was limited to the liquid volume and does not extend into the solid volumes. The temperature simulation space includes the complete volume with constant temperature boundary conditions at the outermost horizontal boundaries ($T_o = 296$ K).

The input power (heating) and output power (fluid power) for each respective heating method was determined. Joule heating and resistive heating are sources of input power for these systems. The total Joule heating power generated from the electrodes was determined with $P_J = \frac{1}{2}\sigma\,|E|^2$, where the magnitude of the electric field, $|E|$, is extracted from the numerical simulation. Resistive heating power (P_R) is a function of the current density, wire resistivity, and film geometry. For this numerical simulation, resistive heating was defined as a 'heat source' input with a user-specified power input (per unit depth, W/m) across the film cross-section.

Fluid energy is proportional to fluid velocity squared, or the square of the volumetric flow rate (Q^2). The flow rate (per unit depth) is determined through the integration of velocity with respect to one of the periodic boundaries within the numerical model. To properly compare the pumping of

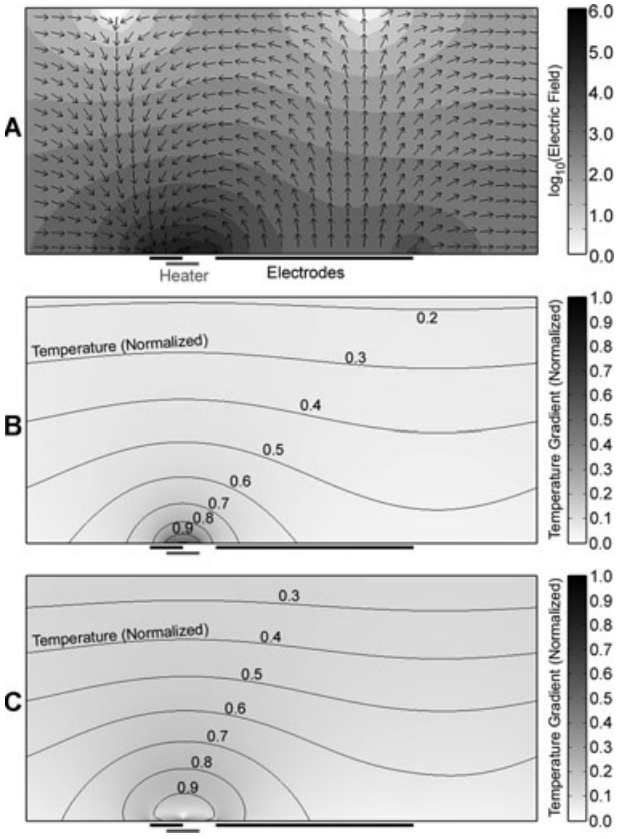

Figure 3. (A) The electric field between the asymmetric electrode array when 1 V is applied. Normalized temperature results for (B) thin film resistive heating and (C) Joule heating.

each independent heating source two electrothermal fluid dynamics models were solved, each one coupled to a respective heating method. The electrothermal flow rate for Joule heating only (Q_J) is compared to the flow rate from resistive heating only (Q_R). Both flows, though, exist simultaneously for this system. The energy generated between these respective methods (Q_R^2 and Q_J^2) will also be compared.

3 Results and discussion

First, a straightforward comparative analysis was conducted to demonstrate the difference in the temperature field gradients between each heating method. The following analysis was conducted with a decoupled model, meaning Eq. (9) was $\nabla^2 V = 0$. Figure 3A shows the electric field between the asymmetric electrode array when 1.0 V is applied between them. Figures 3C shows normalized temperature field (contour lines) and temperature gradients from Joule heating for a fluid with an arbitrary conductivity. Figure 3B shows normalized temperature results for the thin film design with an arbitrary heating input power. Temperature results are normalized with respect to their maximum values as both solutions are scalable with their respective dependent variables for this decoupled analysis. The nature of both temperature fields appears similar, but the thin film heater's normalized temperature field produces sharper gradients closer to the electrode compared to those from Joule heating. The proximity of temperature gradients to the electric field is important as the electrothermal body force exerted on the fluid scales approximately with $\nabla T\, E^2$. Therefore, electrothermal pumps are more efficient with high temperature gradients in close proximity to strong electric fields.

Next, electrothermal flow from both heating methods was compared for identical power inputs. First, the input power from Joule heating was determined for a constant AC voltage of 1.0 V for a fluid conductivity of 1.0 S/m. The resistive thin film heater input power is set at this value, therefore having identical power ($P_R = P_J$). This was repeated for two scenarios, low frequency ($\omega\tau << 1$) and high frequency ($\omega\tau >> 1$). The resultant electrothermal fluid velocity at low frequencies for Joule heating only and resistive heating only are shown in Fig. 4A and B, respectively. Fluid velocity at high frequencies for Joule heating only and resistive heating only are shown in Fig. 4C and D, respectively.

Results from Fig. 4 show that the low frequency regime produces greater net electrothermal flow than high frequencies, regardless of the heating method. High frequency flows generate fluid circulation, but insignificant net flow for this particular electrode geometry. The net pumping rate for high frequencies is approximately one hundred times less than for the low frequency regime, which is consistent with results from Zhang, et al. [24]. The Coulomb force is the dominant electrothermal force component to generate fluid pumping. Therefore, only low frequencies were considered for the proceeding results.

From Fig. 4A and B, electrothermal flow from thin film heating alone is greater than for Joule heating alone. The following quantitative comparisons were performed between Joule heating and thin film resistor electrothermal models having identical power ($P_R = P_J$) at low frequencies ($\omega\tau << 1$): (i) the ratio between their maximum increase in temperature, $T_{max,R}/T_{max,J}$; (ii) the ratio between the product of their temperature gradients with the square of the electric field, $(\nabla T\, E^2)_R/(\nabla T\, E^2)_J$, integrated across the simulation subdomain; (iii) the ratio of the resultant flow rates, Q_R/Q_J; and (iv) the ratio of their efficiencies, Q_R^2/Q_J^2. This comparison is conducted for a range of conductivities (0.1 mS/m to 10 S/m). Results are given in Table 1.

Temperature linearly increases with fluid conductivity except at higher conductivities. At high temperatures, the coupled effects between temperature and electric field cannot be neglected. In addition, ratios remained nearly constant for all fluid conductivities from 0.1 to 0.1 S/m, but change at elevated temperatures. For the same input power the maximum temperature for the thin film heater was approximately 30% greater than Joule heating alone. Also, the electrothermal flow rate from the thin film heater alone was approximately two and one-half times greater than Joule heating alone.

The increased temperature alone ($T_{max,R}/T_{max,J} \approx 1.3$) does not account for the improved electrothermal pumping performance. To demonstrate this, the input power to

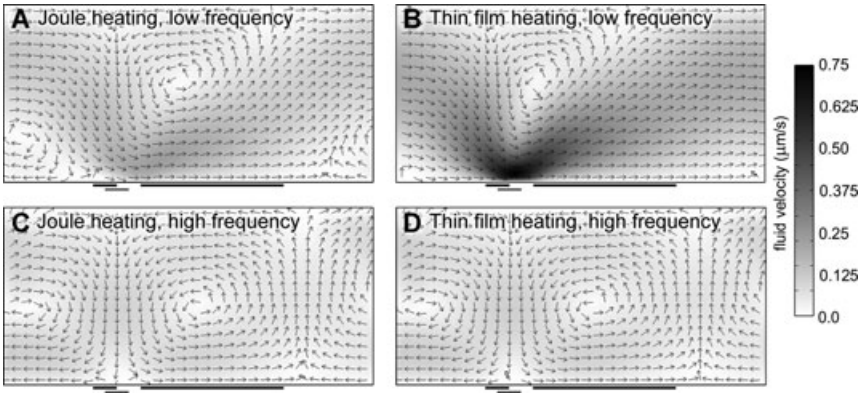

Figure 4. Simulation results of the electrothermal flow at 1.0 V and 1.0 S/m media for (A) Joule heating at low frequency, (B) thin film heating at low frequency, (C) Joule heating at high frequency, and (D) thin film heating at high frequency. The input power for the thin film heater was identical to the power generated from Joule heating ($P_R = P_J$).

Table 1. Numerical simulation results comparing the performance of Joule heating (*J*) and thin film resistive heating (*R*) electrothermal pumps for a range of fluid conductivities.

Conductivity	$T_{max,R}$ (°C)	$T_{max,J}$ (°C)	$T_{max,R}/T_{max,J}$	$(\nabla T E^2)_R/(\nabla T E^2)_J$	Q_R/Q_J	Q_R^2/Q_J^2
0.1 mS/m	0.07×10^{-3}	0.05×10^{-3}	1.31	2.30	2.53	6.40
1.0 mS/m	0.66×10^{-3}	0.50×10^{-3}	1.31	2.30	2.53	6.40
10 mS/m	6.62×10^{-3}	5.04×10^{-3}	1.31	2.30	2.53	6.40
0.1 S/m	66.2×10^{-3}	50.5×10^{-3}	1.31	2.29	2.52	6.35
1 S/m	0.662	0.509	1.30	2.27	2.51	6.30
10 S/m	6.62	5.53	1.20	2.07	2.34	5.48

Results include their resultant maximum temperature (T_{max}), their product of their temperature gradients with the square of the electric field ($\nabla T E^2$), and their flow rates (Q).

the resistive heater (P_R) was decreased until the resultant flow rates from each respective mechanism were identical ($Q_R = Q_P$) for a signal of 1.0 V and fluid conductivity 1.0 S/m. Numerical results show that equal volumetric flow occurs when the input power of the thin film is approximately 40% of that generated through Joule heating ($P_R/P_J = {}^1/_{2.51} = 0.40$) while the maximum temperature increase is approximately one-half ($T_{max,R}/T_{max,J} = 0.52$). These results demonstrate that electrothermal pumping driven with resistive thin films is more efficient than Joule heating methods.

Another advantage of using external thin film heating elements is the ability to use electrothermal fluid pumping independent of fluid conductivity. Joule heating is proportional to σE^2, limiting its application to higher conductivity media. External heating, though, allows electrothermal pumping to occur for low conductivity media. For constant input AC voltage, the resultant input power for Joule heating is minimized at low conductivities. To demonstrate this, a series of numerical simulations were conducted at constant AC voltage (1.0 V) and constant thin film heater input power (P_R = constant) at low frequencies ($\omega\tau << 1$). The thin film heater power is set equal to the resultant Joule heating power (P_J) at 0.1 S/m, this value of P_R is held constant for other conductivities. Figure 5 shows the volumetric flow for each heating component as well as their combined flow (Q_T). All data points are normalized with respect to Q_T at 0.1 S/m. Here, Joule heating electrothermal pumping will dominate at higher conductivities due to higher generated temperatures (hence higher temperature gradients) than the thin film heaters. However, at low conductivities thin film heating dominates resulting in constant

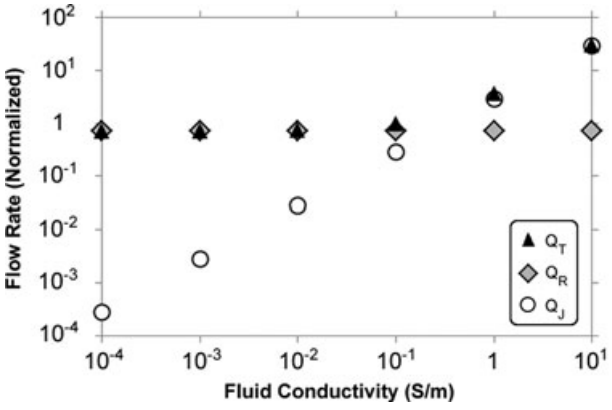

Figure 5. The resultant flow produced from Joule heating (Q_J) and thin film heating (Q_R) at constant P_R and constant AC voltage (1.0 V). All data points are normalized with respect to Q_T at 0.1 S/m.

pumping rates. An electrothermal fluid pump that has constant velocities for a particular range of fluid conductivities is beneficial for precise handling of fluids for micro-analytical systems.

Electrothermal pumps can be optimized through precise placement of resistive heating elements with respect to the electric field. For example, Mizuno et al. (1995) observed fluid recirculation (no net fluid motion) with the placement of a focused laser beam centered between two coplanar electrodes. However, when the heated spot was relocated near the edge of one electrode (closer to larger electric fields), increased fluid

velocities and pumping was observed [17]. The location of nonuniform heating with respect to the electric field dictates the behavior and velocity of electrothermal fluid motion.

The pump analyzed within this manuscript is not an optimized design for thin film electrothermal pumping, but rather a demonstration of the advantages of incorporating thin films for electrothermal flow. For example, if the width of the heating electrode was less than its current dimension of 20 μm, sharper thermal gradients would be generated leading to increased fluid velocities. Similarly, greater electric fields can be generated with AC electrodes of smaller dimensions and spacing. However, nonuniform heating profiles may become more uniform if neighboring resistive heaters are placed in close proximity to each other. Careful analysis of thin film heater placement, design, and heat transfer is necessary.

The use of thin film heaters will lead to novel electrothermal pump designs that are impossible with Joule heating methods. For example, an interdigitated array of symmetric electrodes would produce electrothermal circulation, but no net fluid motion. With proper incorporation of thin film heaters, net pumping can be achieved. Further, the thin film heaters are controlled independently. Therefore, pumping actuation is independently addressable, leading to stepwise procedures and multipurpose AC electrode functionality. For example, a symmetric interdigitated array may concentrate a colloidal sample with dielectrophoresis then, with the activation of embedded heaters, can pump the sample downstream. Further, sets of addressable heaters can guide the sample to a location within the microsystem with controlled electrothermal hydrodynamics.

In addition, electrothermal pumping can occur in a uniform electric field environment. Nonuniform heating is generated from the heater elements, whereas a uniform electric field would generate negligible temperature gradients. Therefore electrothermal actuation can be integrated with uniform electric field techniques like electrophoresis or electro-osmosis. Recently, V. Velasco and S.J. Williams [28] incorporated thin film heaters within a uniform electric field environment to concentrate, pattern, and sort colloids.

The use of thin film heaters may improve the performance of out-of-phase electrothermal pumps [3, 24, 25]. Zhang, et al. [24], demonstrated that a two-phase electrothermal pump can achieve up to 50% faster flow rates than single-phase pumps of the same electrode geometry. Results herein, using the same electrode geometry, has shown that heat generated from resistive elements alone can generate approximately two and one-half times greater electrothermal volumetric flow than Joule heating alone.

4 Concluding remarks

This work communicated the concept of using embedded thin films for the advancement of electrothermal pump design. This method is more efficient than Joule heating based electrothermal pumping alone. The external heating mechanism allows pumping of low conductivity media. Thin film heaters are independently addressable, providing a degree of control for electrohydrodynamic pumping and mixing. The use of thin film heaters for electrothermal pumping improves device performance, resulting in reduced AC voltages or decreased fluid heating. New applications of electrothermal pumping are possible with the incorporation of external heating with thin films.

S. J. Williams acknowledges the support from start-up funds from the University of Louisville. This author acknowledges valuable conversations with Sophie Loire regarding her recent work in electrothermal flow numerical simulations [4, 23].

The author has declared no conflict of interest.

5 References

[1] Green, N. G., Ramos, A., Gonzalez, A., Castellanos, A., Morgan, H., *J. Phys. D Appl. Phys.* 2000, *33*, L13–L17.

[2] Green, N. G., Ramos, A., Gonzalez, A., Castellanos, A., Morgan, H., *J. Electrostat.* 2001, *53*, 71–87.

[3] Gonzalez, A., Ramos, A., Morgan, H., Green, N. G., Castellanos, A., *J. Fluid. Mech.* 2006, *564*, 415–433.

[4] Loire, S., Kauffmann, P., Mezic, I., Meinhart, C. D., *J. Phys. D Appl. Phys.* 2012, *45*, 185301.

[5] Ajdari, A., *Phys. Rev. E* 2000, *61*, R45-R48.

[6] Muller, T., Gerardino, A., Schnelle, T., Shirley, S. G., Bordoni, F., DeGasperis, G., Leoni, R., Fuhr, G., *J. Phys. D Appl. Phys.* 1996, *29*, 340–349.

[7] Ramos, A., Morgan, H., Green, N. G., Castellanos, A., *J. Phys. D Appl. Phys.* 1998, *31*, 2338–2353.

[8] Trau, M., Saville, D. A., Aksay, I. A., *Langmuir* 1997, *13*, 6375–6381.

[9] Cahill, B. P., Heyderman, L. J., Gobrect, J., Stemmer, A., *Phys. Rev. E* 2004, *70*, 036305.

[10] Studer, V., Pepin, A., Chen, Y., Ajdari, A., *Analyst* 2004, *129*, 944–949.

[11] Green, N. G., Ramos, A., Gonzalez, A., Morgan, H., Castellanos, A., *Phys. Rev. E* 2000, *61*, 4011–4018.

[12] Green, N. G., Ramos, A., Gonzalez, A., Morgan, H., Castellanos, A., *Phys. Rev. E.* 2002, *66*, 026305.

[13] Castellanos, A., Ramos, A., Gonzalez, A., Green, N. G., Morgan, H., *J. Phys. D Appl. Phys.* 2003, *36*, 2584–2597.

[14] Fuhr, G., Mueller, T., Baukloh, V., Lucas, K., *Hum. Reprod.* 1998, *13*, 136–141.

[15] Kumar, A., Williams, S. J., Wereley, S. T., *Microfluid. Nanofluid.* 2009, *6*, 637–646.

[16] Mizuno, A., Nishioka, M., Ohno, Y., Dascalescu, L. D., *IEEE T. Ind. Appl.* 1995, *31*, 464–468.

[17] Nakano, M., Katsura, S., Touchard, G. G., Takashima, K., Mizuno, A. *IEEE T. Ind. Appl.* 2007, *43*, 232–237.

[18] Laser, D. J., Santiago, J. G., *J. Micromech. Microeng.* 2004, *14*, R35–R64.

[19] Liao, C.-S., Lee, G.-B., Wu, J.-J., Chang, C.-C., Hsieh, T.-M., Huang, F.-C., Luo, C.-H., *Biosens. Bioelectron.* 2005, *20*, 1341–1348.

[20] Semancik, S., Cavicchi, R. E., Wheeler, M. C., Tiffany, J. E., Poirier, G. E., Walton, R. M., Suehle, J. S., Panchapakesan, B., DeVoe, D. L., *Sensor. Actuat. B Chem* 2001, *77*, 579–591.

[21] Sunding, J., Williams, S. J., Electrothermal Pumping with Thin Film Resistive Heaters, ASME/IMECE, Denver, CO, USA, 2011.

[22] Melcher, J. R., *Continuum Electromechanics*, MIT Press, Cambridge, MA, 1981.

[23] Loire, S., Kauffmann, P., Mezic, I., *COMSOL Conference*. Boston, MA, USA, 2011 .

[24] Zhang, R., Dalton, C., Jullien, G. A., *Microfluid. Nanofluid.* 2011, *10*, 521–529.

[25] Perch-Nielsen, I. R., Green, N. G., Wolff, A., *J. Phys. D Appl. Phys.* 2004, *37*, 2323–2330.

[26] White, F. M., *Fluid Mechanics*, 5th ed. McGraw-Hill, New York, NY, 2003.

[27] Wu, J., Lian, M., Yang, K.,. *Appl. Phys. Lett.* 2007, *90*, 234103.

[28] Velasco, V., Williams, S. J., *J. Colloid Interf. Sci.* 2013, *394*, 598–603.

